Low-power radio frequency amplification module with dynamic tunable notch filters for the Antarctic Impulsive Transient Antenna (ANITA)

P. Allison,[1,2] O. Banerjee*,[1,2] L. Batten,[3] J. J. Beatty,[1,2] K. Belov,[4] D. Z. Besson,[5] W. R. Binns,[6] V. Bugaev,[6] P. Cao,[7] C. Chen,[8] P. Chen,[8] J. M. Clem,[7] A. Connolly,[1,2] L. Cremonesi,[3] B. Dailey,[1] C. Deaconu,[9] P. F. Dowkontt,[10] P. W. Gorham,[11] J. Gordon,[1] B. Hill,[11] R. Hupe,[1] M. H. Israel,[6] M. Kovacevich,[1] J. Kowalski,[11] J. Lam,[10] J. G. Learned,[11] K. M. Liewer,[4] T. C. Liu,[8] A. Ludwig,[9] S. Matsuno,[11] C. Miki,[11] K. Mulrey,[7] J. Nam,[8] R. J. Nichol,[3] A. Novikov,[5,12] E. Oberla,[9] S. Prohira,[5] B. F. Rauch,[6] J. Roberts,[11] A. Romero-Wolf,[4] B. Rotter,[11] J. Russell,[11] D. Saltzberg,[10] D. Seckel,[7] S. Stafford,[1] J. Stockham,[5] M. Stockham,[5] B. Strutt,[3] K. Tatem,[11] G. S. Varner,[11] A. G. Vieregg,[9] S. A. Wissel,[13] F. Wu,[10] and R. Young[5]

[1]*Dept. of Physics, Ohio State Univ., Columbus, OH 43210.*
[2]*Center for Cosmology and AstroParticle Physics, Ohio State Univ., Columbus, OH 43210.*
[3]*Dept. of Physics and Astronomy, University College London, London, United Kingdom.*
[4]*Jet Propulsion Laboratory, Pasadena, CA 91109.*
[5]*Dept. of Physics and Astronomy, Univ. of Kansas, Lawrence, KS 66045.*
[6]*Dept. of Physics, Washington Univ. in St. Louis, MO 63130.*
[7]*Dept. of Physics, Univ. of Delaware, Newark, DE 19716.*
[8]*Dept. of Physics, Grad. Inst. of Astrophys., Leung Center for Cosmology and Particle Astrophysics, National Taiwan University, Taipei, Taiwan.*
[9]*Dept. of Physics, Enrico Fermi Institute, Kavli Institute for Cosmological Physics, Univ. of Chicago , Chicago IL 60637.*
[10]*Dept. of Physics and Astronomy, Univ. of California, Los Angeles, Los Angeles, CA 90095.*
[11]*Dept. of Physics and Astronomy, Univ. of Hawaii, Manoa, HI 96822.*
[12]*National Research Nuclear University, Moscow Engineering Physics Institute, 31 Kashirskoye Highway, Rossia 115409*
[13]*Dept. of Physics, California Polytechnic State Univ., San Luis Obispo, CA 93407.*

(Dated: April 10, 2017)

The Antarctic Impulsive Transient Antenna (ANITA) is a NASA long-duration balloon mission with the primary goal of Askaryan radio detection of ultra-high-energy neutrinos. The fourth ANITA mission, ANITA-IV, recently flew from Dec 2, 2016 through Dec 29, 2016. The most significant change in signal processing in ANITA-IV was the inclusion of the Tunable Universal Filter Frontend (TUFF) boards. The TUFF boards had a three-fold purpose as follows: a) second-stage amplification by 45 dB to boost the $\sim \mu$V-level radio frequency (RF) signals to $\sim$ mV-level for digitization; b) mitigation of narrow-band, anthropogenic noise with tunable, switchable RLC notch filters and c) supplying power via bias tees to the first-stage, antenna-mounted amplifiers. To accomplish this with a < 1 kW total power budget and highly constrained space and weight requirements of a balloon mission, the TUFF boards needed to be low-power, compact and light. Sixteen TUFF boards were built to serve six ANITA channels each with a per-channel power consumption of 330 mW. Eight pairs of TUFF boards were each assembled into a final 12-channel aluminum housing to provide heat-sinking, structural support, and RF isolation. During the ANITA-IV mission, these eight, 12-channel modules, for a total of 96 channels, were successfully operated throughout the flight. In this paper, we outline the design and performance of the TUFF boards during the ANITA-IV flight and plans for improving the boards for ANITA-V.

I. INTRODUCTION

The Antarctic Impulsive Transient Antenna (ANITA) is a NASA long-duration balloon-borne radio experiment for the detection of ultra-high energy (UHE) neutrinos using the Antarctic ice as its detection volume. UHE neutrinos would interact in the ice, producing an electromagnetic cascade that develops a charge asymmetry and emits a coherent Cherenkov radio impulse extending to ~ 1 GHz via the Askaryan effect [1]. The radio impulses received at the payload are at the level of thermal emission from the Antarctic ice ($\sim 20\,\mu$V).

Following thermal radiation, ANITA's dominant source of noise is human-made narrow-band transmissions, henceforth referred to as continuous-wave (CW) interference. While Antarctica itself is relatively free of CW transmissions, except for bases of human activity, transmissions from geosynchronous satellites are continuously in view because the beam of the ANITA antennas extends to the horizontal and above. The Antarctic science bases such as McMurdo

* Corresponding author.
E-mail: oindreeb@gmail.com | Tel.: +1 (614) 800-4409

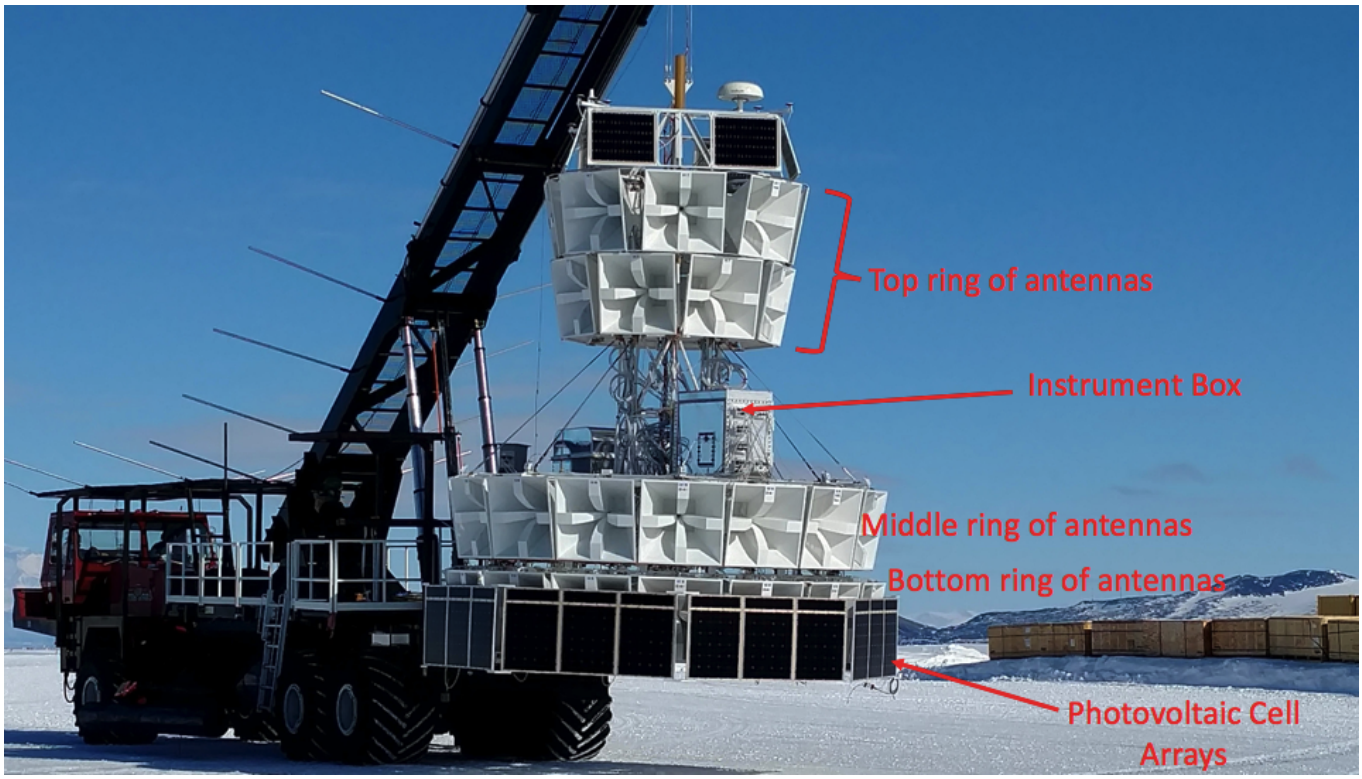

FIG. 1: The ANITA-IV payload just prior to launch at NASA LDB Facility near McMurdo Station, Antarctica.

Station, South Pole Station, etc. are much radio-louder than the rest of the continent, producing CW interference, for example, in the $\sim 430 - 460$ MHz band.

CW interference due to military satellites has been problematic for all past flights of ANITA, but especially detrimental to the ANITA-III flight. ANITA-I and ANITA-II observed CW interference primarily in the $240 - 270$ MHz band, peaking at ~ 260 MHz. This frequency range is predominantly used by the aging Fleet Satellite (FLTSAT) Communications System and Ultra High Frequency Follow-On (UFO) System, both serving the United States Department of Defense. Lesser interference was also seen at approximately ~ 380 MHz, which is presumed to be the newer Mobile User Objective System (MUOS) satellites. Because of the design of the ANITA-I and ANITA-II trigger, which required coincidences among different frequency bands, the CW interference did not overwhelm the acquisition system. However, the ANITA-III trigger, which was redesigned to trigger on full-bandwidth signals for improved sensitivity, produced trigger rates far in excess of the acquisition system's readout capabilities (~ 50 Hz) for thresholds comparable to those used in previous flights. This forced us to increase our thresholds in the presence of CW interference and sacrifice some neutrino sensitivity during those periods.

Mitigation of CW interference, especially due to military satellites, is critical to the ANITA experiment. In ANITA-III, "phi-masking" was used during noisy periods to veto triggers from approximately half of the payload field-of-view to keep the trigger rate at or below 50 Hz. To restore triggering efficiencies in the presence of CW interference, tunable notch filters were built for the ~ 260 MHz (Notch 1), ~ 380 MHz (Notch 2) and ~ 460 MHz (Notch 3) bands.

II. ANITA-III AND IV TRIGGER SYSTEMS

The ANITA-III and IV payloads primarily consist of the following components: a) 48 dual-polarized, highly directional (on-axis gain of ~ 10 dBi, 3 dB point averaged over in-band frequencies is $\sim 30°$) horn antennas, b) an Instrument Box containing different units for signal processing (illustrated for ANITA-IV in Figure 2) c) a NASA Science Instrument Package, d) a Battery Box, e) three GPS systems and f) photovoltaic cells for solar-powering the payload. The 12-channel TUFF modules reside inside four Internal Radio Frequency Conditioning Modules (IRFCMs) inside the ANITA-IV Instrument Box. Figure 1 shows the ANITA-IV payload just prior to launch at NASA Long Duration Balloon (LDB) Facility near McMurdo Station.

For each ANITA channel, RF signal is processed and digitized in the Instrument Box as illustrated in Figure 2

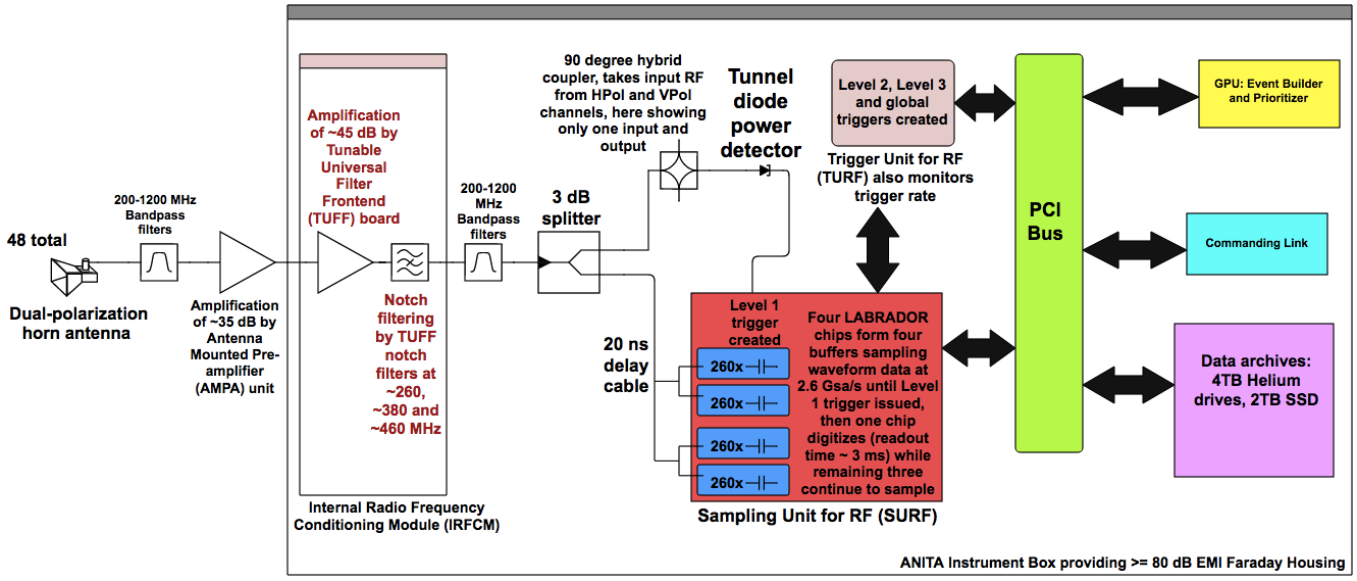

FIG. 2: The ANITA-IV signal processing chain for a single RF channel.

(ANITA-IV). Since the ANITA-III and IV payloads each has 48 dual-polarized antennas, there are total 96 RF channels for these flights. A tunnel diode acts as a square-law power detector for each RF channel. Following the tunnel diode, the RF signal is sampled by four LABRADOR chips (buffers) each consisting of a 260-element switched capacitor array, in the Sampling Unit for Radio Frequency (SURF). The tunnel diode and the SURF are together responsible for issuing the Level 1 trigger when the power in a channel exceeds a certain threshold. When the Level 1 trigger is issued, one LABRADOR chip digitizes the signal, while the remaining three continue to sample.

The ANITA antennas (48 total) are mounted on three rings: bottom, middle and top, forming 16 azimuthal sectors or phi sectors of antennas (as shown in Figure 1). If RF signal in a top ring antenna exceeds the threshold, then the middle and bottom antennas are checked for excess in the previous 8 and 12 ns respectively, or if a middle ring antenna has signal exceeding the threshold, then the bottom ring antenna is checked in the previous 4 ns. This process could issue Level 1 triggers for an entire phi sector of antennas consisting of a top, a middle and a bottom ring antenna. A Level 3 trigger is issued when Level 1 triggers are issued in adjacent phi sectors of antennas. This is how the trigger works in ANITA-III.

In ANITA-IV, there is an additional requirement that the signal must contain equal parts of left and right circular polarization (LCP and RCP) components, before a Level 1 trigger can be issued. This would increase the probability of the signal being linearly polarized, and thus it would be more likely to come from a neutrino or cosmic-ray source.

During the ANITA-III flight, when the payload was strongly hit with anthropogenic noise or CW interference from a particular direction, the triggers from phi sectors on that side of the payload, covering approximately half of the payload field-of-view, were vetoed, and this was called "phi-masking".

III. TUFF BOARD DESIGN

The total power budget of the ANITA payload is < 1 kW. Moreover, there are severe restrictions on weight and space for a balloon mission. Thus, the TUFF boards needed to be low-power, compact and light. Figure 3 shows a single TUFF channel next to a quarter USD coin for size comparison.

We built and deployed 16 TUFF boards total (not counting spares) with six channels each for the 96 total RF channels of ANITA. Each channel consumed only 330 mW of power. Two TUFF boards (even and odd serial numbered) were assembled into a final 12-channel aluminum housing to provide heat-sinking, structural support, and RF isolation. Two of these 12-channel modules were placed inside an IRFCM inside the Instrument Box of ANITA. Figure 4 shows the inside of an IRFCM.

Each TUFF channel has three main components and functions: a) a bias tee to power the first-stage antenna-mounted amplification unit, b) two amplifiers that together produce second-stage RF power amplification of ~ 45 dB and c) three tunable, switchable notch filters that can be controlled during flight using the channel's microcontroller for mitigation of CW noise at ~ 260 MHz (Notch 1), ~ 380 MHz (Notch 2) and ~ 460 MHz (Notch 3). Figure 3 shows

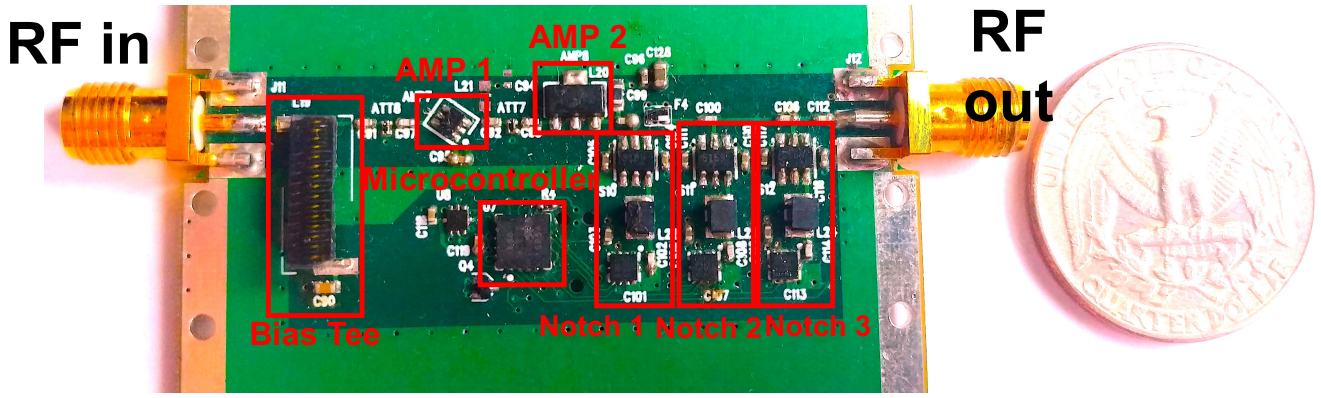

FIG. 3: This is an image of a single TUFF board unit or channel that powers the first-stage antenna-mounted amplification unit and performs second-stage amplification and notch filtering of a single RF channel (out of 96 total). Each TUFF board has six such channels. The main components of the channel are highlighted here.

a single channel and its main components.

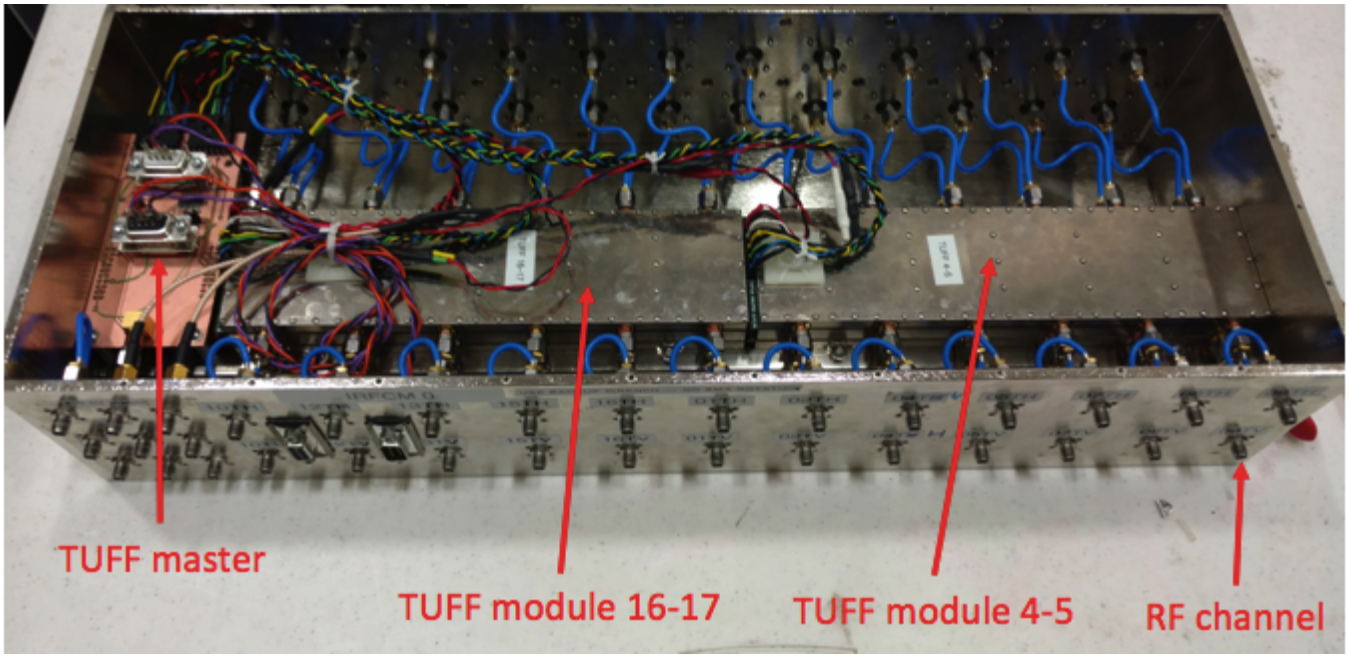

FIG. 4: Internal Radio Frequency Conditioning Module (IRFCM) containing two 12 channel TUFF modules serving 24 RF channels total, together with a TUFF Master for communication with the TUFFs from Flight Computer.

Each TUFF notch filter is an RLC circuit. The resistance R is a parasitic resistance of $\sim 6 - 7\,\Omega$. The inductance L is fixed at 56 nH. The capacitance C comes from a variable capacitor (Peregrine Semiconductor, part number PE64906) in parallel with a $0.1\,\mu$F decoupling capacitor. The variable capacitor can be tuned in discrete steps of 119 fF in the range $0.9 - 4.6$ pF. For Notch 1, the variable capacitor is also in parallel with a 2.4 pF capacitor. For Notch 2 and 3, the variable capacitor is in series with a 5.0 pF (Notch 2) and a 2.4 pF (Notch 3) capacitor for increased tuning capability. Figure 5 shows a circuit diagram.

The TUFF notches were able to achieve power attenuation of ~ 13 dB. With the tuning capability of the variable capacitor, the resonant frequency of the RLC circuit could be modified during flight to dynamically mitigate CW interference.

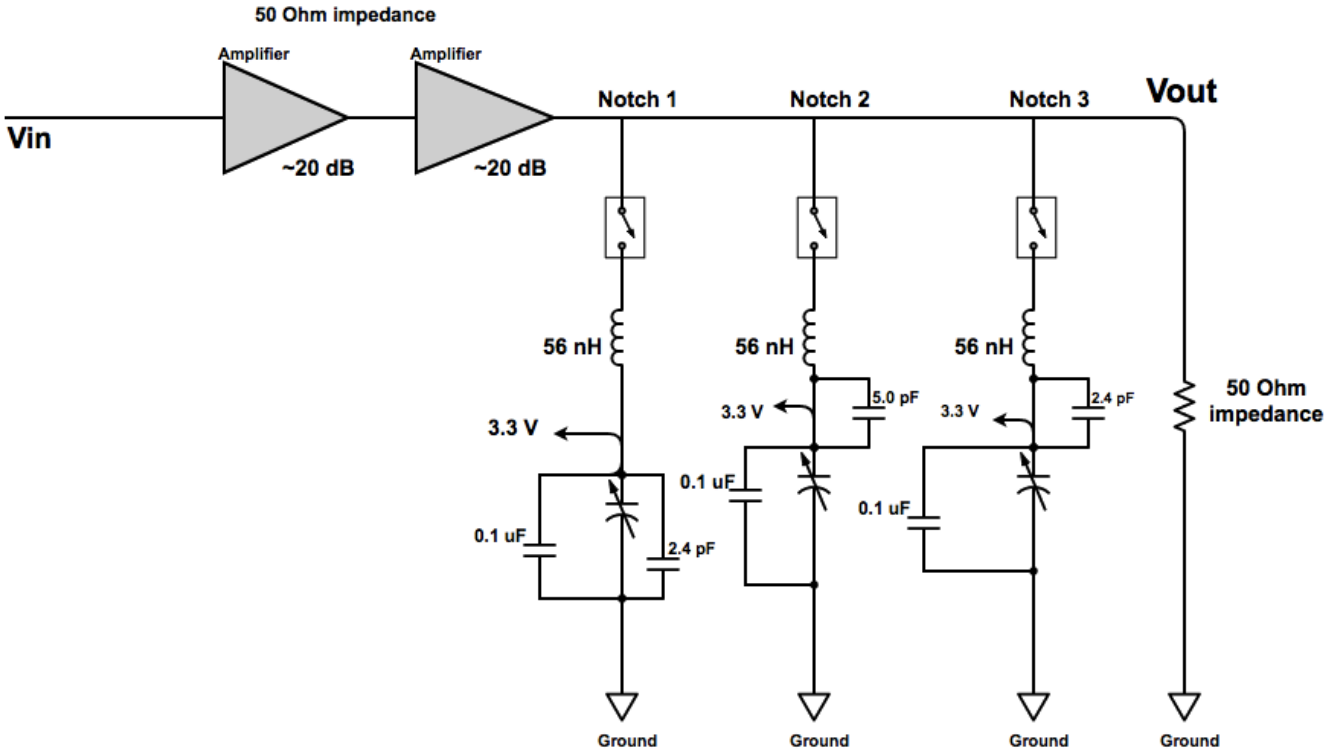

FIG. 5: Circuit diagram showing the different components of the TUFF notch filters.

IV. TUFF BOARD PERFORMANCE

The TUFF boards were deployed for the first time in the ANITA-IV mission. Figure 2 shows, for a single RF channel in ANITA-IV, where the TUFF boards are in the signal processing chain. The ANITA-IV payload was launched on Dec 2, 2016 from NASA LDB Facility located ~ 10 km from McMurdo Station in Antarctica. The flight was terminated on Dec 29, 2016 and landed approximately 100 km from the South Pole. In Figures 10 through 14, the shaded regions indicate when the ANITA-IV payload was in line of sight of the NASA LDB Facility. At these times, increased CW signal is expected.

The main improvement of the ANITA-IV mission over the ANITA-III mission is its superior handle on anthropogenic noise or CW interference . This was done through two methods: a) dynamic CW noise filtering with the TUFF boards and b) requiring coincidence of left and right circular polarization (LCP and RCP) for triggered events. In this paper, we discuss the performance of the TUFF boards during the ANITA-IV flight.

During the ANITA-III flight, a CW signal at ~ 260 MHz from military satellite systems (CW peak seen in Figure 6) was present throughout the flight. This CW signal was omnipresent during the ANITA-IV flight as well, and so Notch 1 needed to be active the whole time. Notch 1 (usually centered at ~ 260 MHz) was re-tuned on Dec 14 to filter the ~ 250 MHz frequency region and was tuned back to 260 MHz later that day.

During the ANITA-III flight, a second CW peak at ~ 370 MHz from military satellite systems (CW peak seen in Figure 6) was present most of the time. In ANITA-IV, too, this CW noise was present. During the ANITA-IV flight, Notch 2, although de-activated twice (Dec 2, Dec 19), needed to be activated again within minutes. After being de-activated on Dec 2 for ~ 16 minutes, Notch 2 needed to be activated again. Excess CW noise upon de-activating Notch 2 was seen in almost all phi sectors. In Figure 7 we show spectra averaged over all waveforms from one phi sector. Notch 2 was de-activated again on Dec 19 for a few minutes but needed to be activated again as excess CW noise was seen in several phi sectors.

Notch 2 was re-tuned during flight a few times (Dec 6-8) to dynamically combat CW interference in the range of $\sim 360 - 390$ MHz. Figure 8 shows the effect of realtime tuning of Notch 2 on Dec 7 for mitigation of CW interference at ~ 390 MHz. Tuning the notch brought the CW noise power down.

Notch 3 was generally activated when the payload was in view of Antarctic bases and filtered the $\sim 450 - 460$ MHz frequency region. Notch 3 was de-activated on Dec 2 for a few minutes but had to be activated again as the payload was close to McMurdo Station at the time. Figure 9 summarizes whether each notch was activated or not as a function

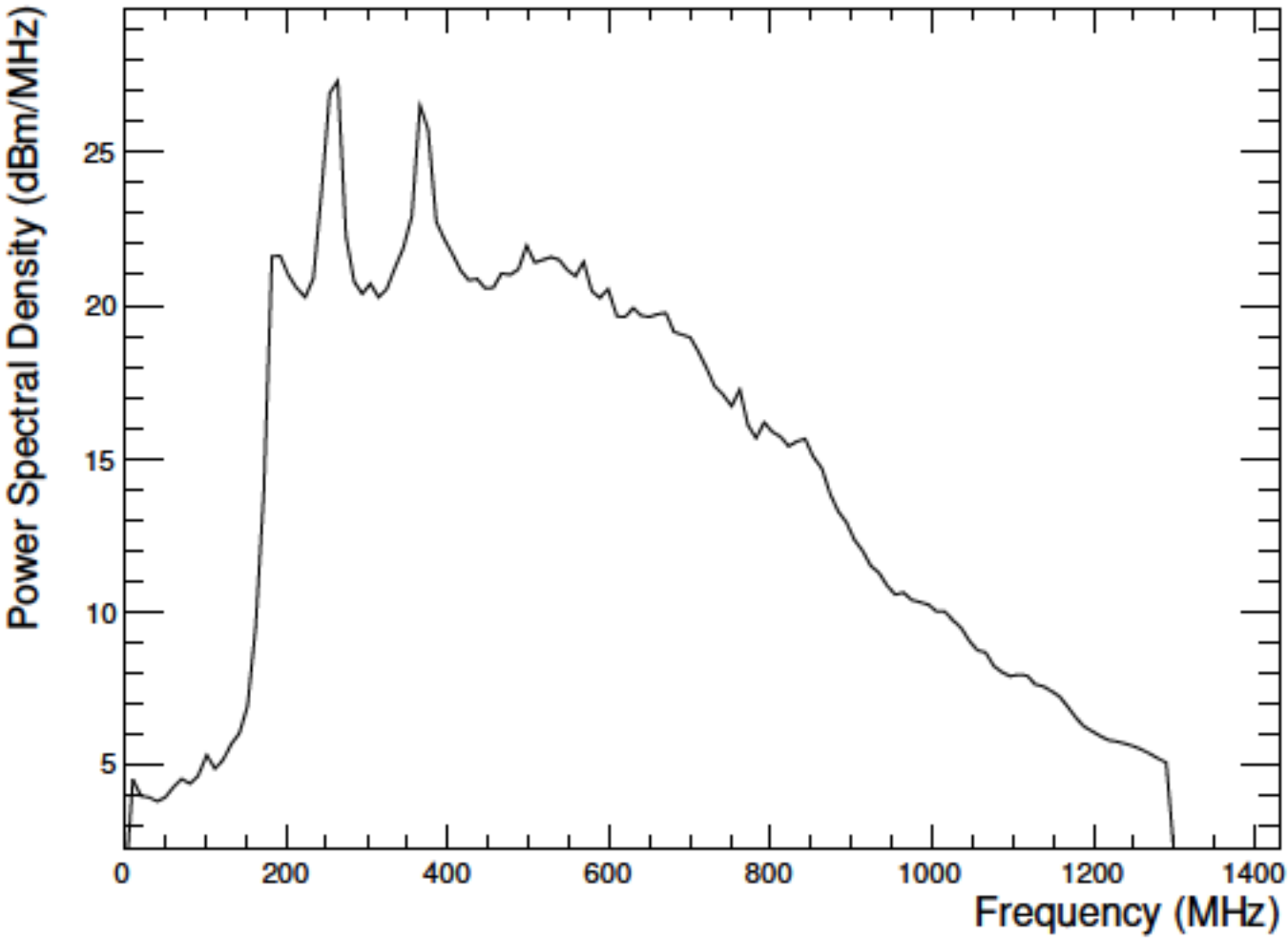

FIG. 6: This shows for a single channel the average power spectral density over ~ 1 min from when the ANITA-III payload was near WAIS Divide in Antarctica. The two peaks at ~ 260 MHz and ~ 370 MHz, presumably from military satellites, are visible here. The ~ 260 MHz peak was present throughout the flight and the ~ 370 MHz peak for most of the flight. These CW peaks motivated the installation of the TUFF notch filters in ANITA-IV. As it turns out, Notch 1 (to curb the left peak) and Notch 2 (to curb the right peak) both needed to be active for practically the whole flight in ANITA-IV.

of time since launch.

Masking in azimuth or phi-masking was needed much less often during the ANITA-IV flight compared to ANITA-III, as seen in Figure 10.

In ANITA, waveforms are only written down when they pass a certain threshold, expressed in DAC (digital to analog converter) counts, of output from the tunnel diode square-law power detector shown in Figure 2. Lower this threshold is the more sensitive ANITA is to weaker neutrino signals. Thresholds were mostly kept constant during the ANITA-IV flight as compared to ANITA-III. Although, the average threshold value in ANITA-IV is higher than that in ANITA-III, as seen in Figure 11, this is because of the LCP and RCP coincidence requirement of the ANITA-IV trigger. To take out the effect of the LCP and RCP coincidence, for comparison between the two flights, one would multiply the ANITA-III thresholds by $\sqrt{2}$. Keeping thresholds constant and lower translate to maintaining a steadier and higher sensitivity for neutrino detection throughout the flight.

Typically, the target trigger rate in ANITA is $20 - 50$ Hz. ANITA triggers on thermal noise at approximately this rate. When the trigger rate is much above this, it typically means that the instrument is getting inundated by CW noise. This leads to instrument deadtime and inability to perform neutrino science. Trigger rate varied less in ANITA-IV as seen in Figure 12. A more stable trigger rate (in the target range) translates to increased livetime and thus higher probability of discovering neutrinos.

Increasing instrument livetime was the primary motivation behind building and deploying the TUFF boards in ANITA-IV. In ANITA, deadtime due to digitization by all four buffers of the SURF is recorded by the Triggering

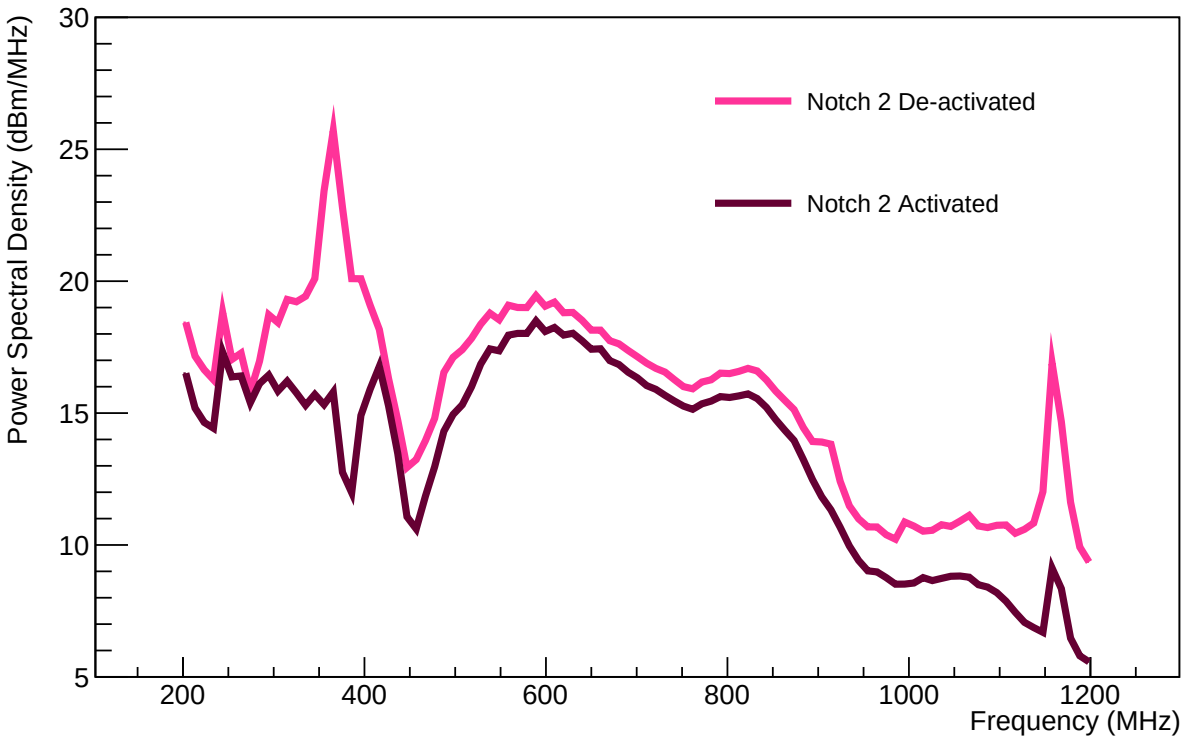

FIG. 7: This figure shows power spectra with Notch 2 de-activated and Notch 2 activated (spectra averaged over 16.5 minutes) during the ANITA-IV flight. Notch 2 was de-activated on Dec 2 for 16 minutes with the result of a CW peak seen in the spectra. So Notch 2 was activated again. With Notch 2 active, the CW peak is curbed. Although we show only phi sector 16 here, excess CW noise upon de-activating Notch 2 and the effect of activating Notch 2 again was seen in almost all phi sectors.

Unit for Radio Frequency (TURF) unit, illustrated in Figure 2. This deadtime is recorded as a fraction of a second. Digitization livetime per second can be obtained by subtracting this from one. Digitization livetime is shown for ANITA-III and ANITA-IV in Figure 13. The total digitization livetime for ANITA-III and ANITA-IV was calculated to be 85.1% and 94.2% respectively.

The TUFF boards helped to not only increase the total digitization livetime, but also the total instrument livetime. For a particular time, this digitization livetime multiplied by the corresponding fractional unmasked phi sectors, obtained by dividing phi-masking by 16 and then subtracting from one, gives us the instrument livetime per second. This is shown for ANITA-III and ANITA-IV in Figure 14. The total instrument livetime for ANITA-III and ANITA-IV was calculated to be 31.6% and 91.3% respectively. Sensitivity of the instrument for neutrino detection is directly proportional to livetime, and therefore, the ANITA-IV instrument was $\sim$ 60% more sensitive than the ANITA-III instrument.

V. PLANS FOR ANITA-V

For the next proposed ANITA mission, ANITA-V, we would like to prioritize building improved hardware for other RF signal digitization and triggering units. It was critical that the TUFF boards perform well during ANITA-IV for a number of reasons. The TUFF boards enabled a high livetime and higher trigger efficiency than we would have had without them in ANITA-IV. For ANITA-V, having established a mechanism to mitigate the effects of CW interference allows us to focus on improving other parts of the signal processing chain, such as, increasing the number of buffers in the Sampling Unit for Radio Frequency (SURF) shown in Figure 2 for less deadtime due to digitization. Modifications to the TUFF boards in ANITA-V will mainly focus on improving mechanical durability of the boards with regard to how they are accommodated in the Instrument Box and how they connect to the rest of the signal chain.

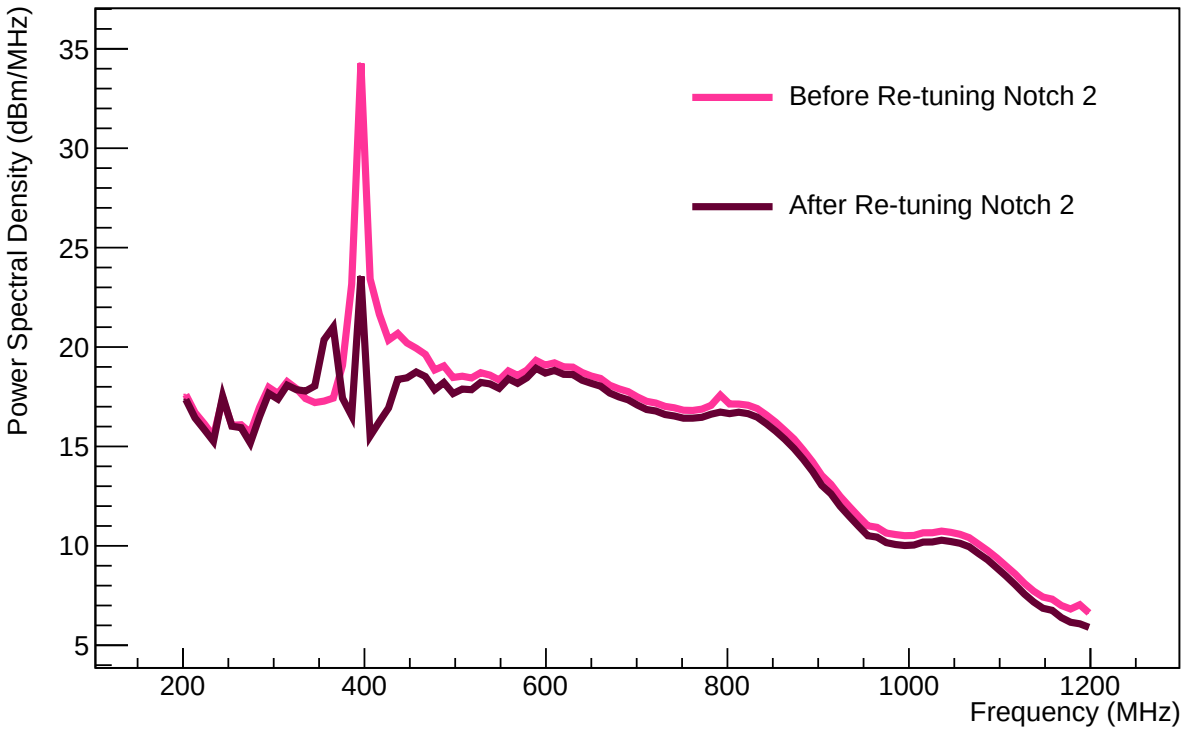

FIG. 8: This figure shows power spectra (averaged over 2 hours) from before and after dynamically tuning Notch 2 during the ANITA-IV flight. On observing large CW peak at $\sim$ 390 MHz on Dec 7, Notch 2 was re-tuned. Although we show only phi sector 8 here, similar CW peak and notch tuning effects were seen in all phi sectors.

VI. ACKNOWLEDGMENTS

We thank NASA for their generous support of ANITA, and the Columbia Scientific Balloon Facility for their excellent field support, and the National Science Foundation for their Antarctic operations support. This work was also supported by the US Dept. of Energy, High Energy Physics Division.

VII. REFERENCES

[1] G. A. Askar'yan, "Excess negative charge of an electron-photon shower and its coherent radio emission," *Sov. Phys. JETP*, vol. 14, no. 2, pp. 441–443, 1962. [Zh. Eksp. Teor. Fiz.41,616(1961)].

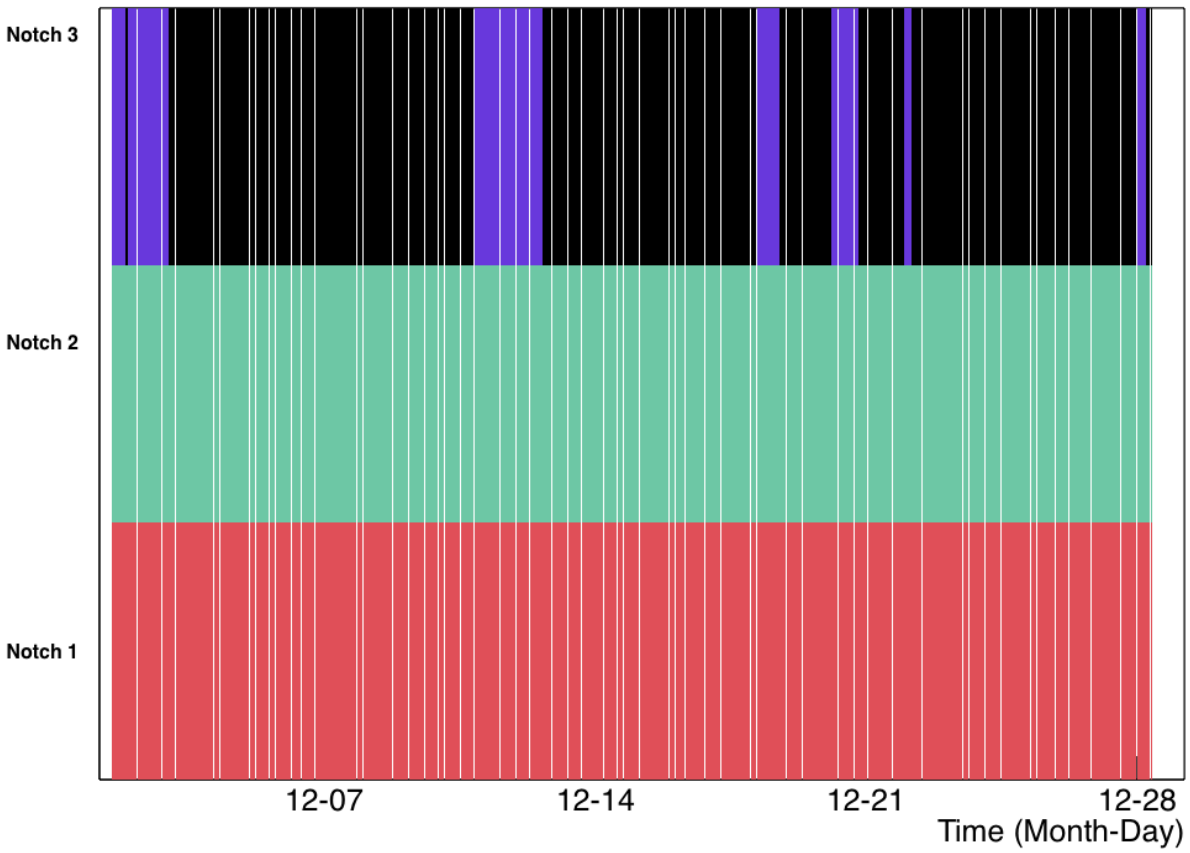

FIG. 9: This figure shows the activated (red for Notch 1, green for Notch 2, blue for Notch 3) or de-activated (black) status for each TUFF notch filter during the flight. The thin white stripes are where timing data is missing.

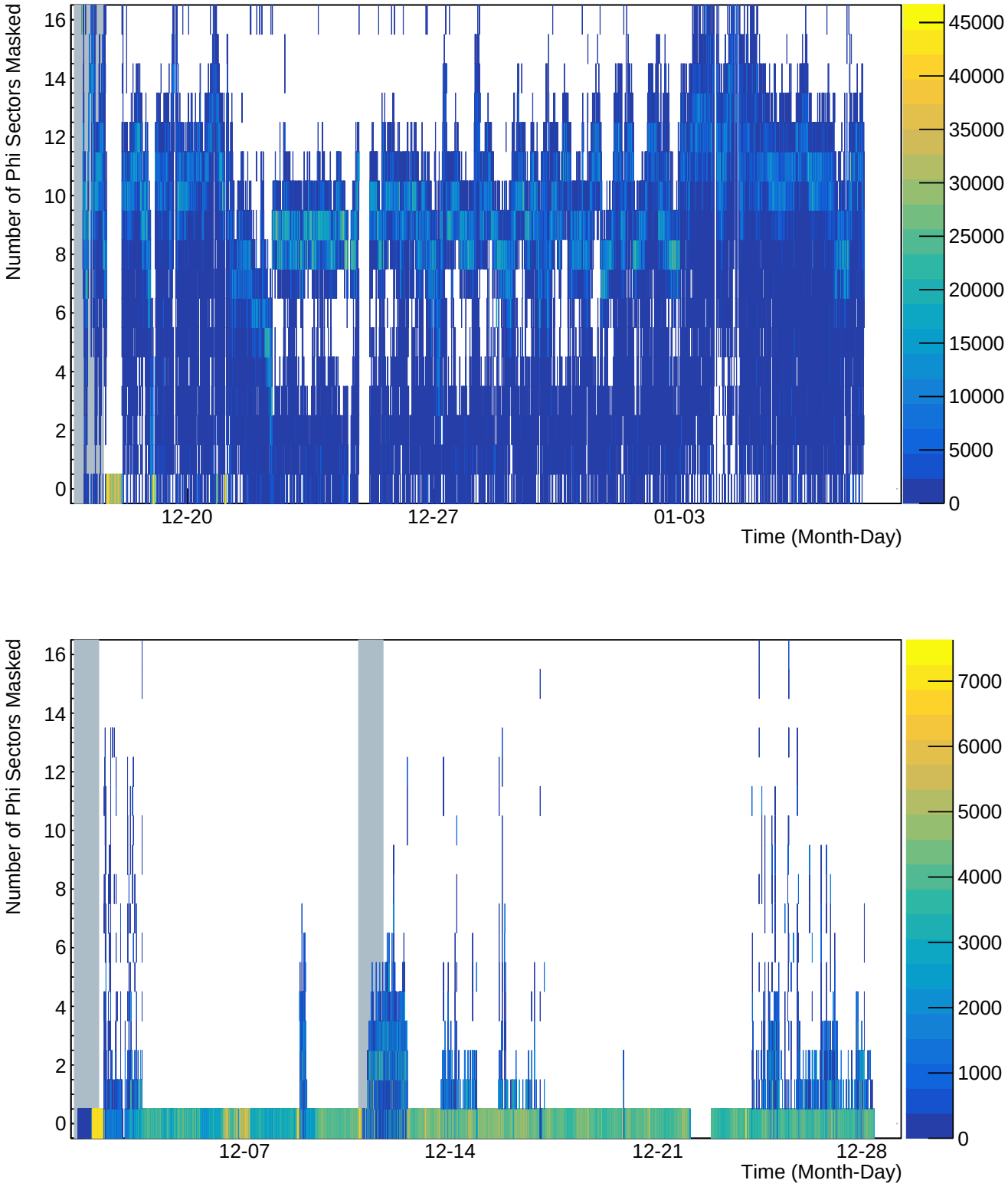

FIG. 10: Phi-masking in the ANITA-III (top) and ANITA-IV (bottom) flights. Because of mitigation of CW noise by the TUFF notch filters, phi-masking needed to be implemented less often in ANITA-IV.

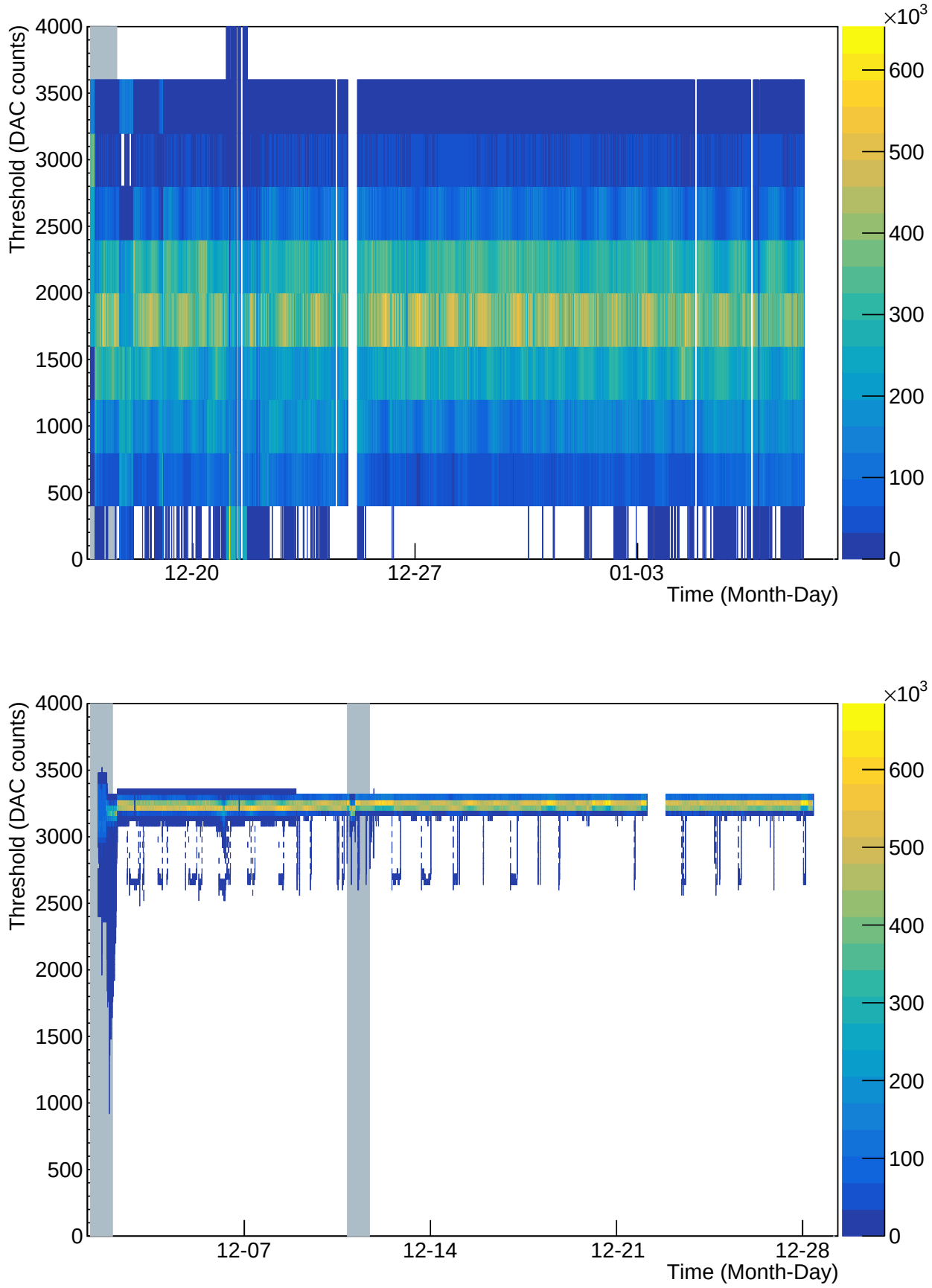

FIG. 11: Thresholds in DAC counts for the ANITA-III (top) and ANITA-IV (bottom) flights. Because of superior handle on CW interference by the TUFF boards, thresholds did not need to be changed as much during the ANITA-IV flight.

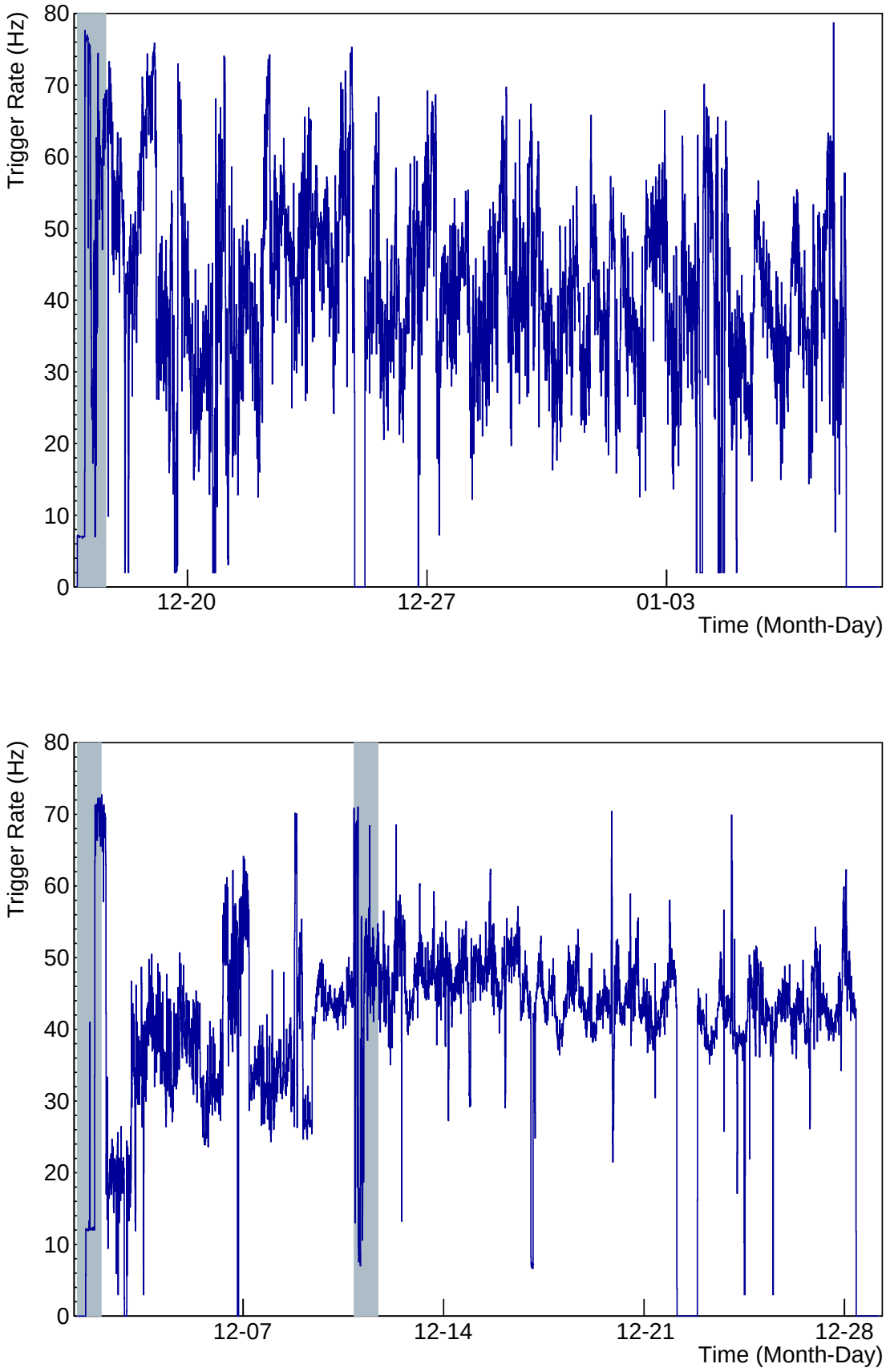

FIG. 12: Trigger rate, averaged over 10 minutes, for ANITA-III (top) and ANITA-IV (bottom). The TUFF boards helped to keep the trigger rate in ANITA-IV more steady compared to ANITA-III.

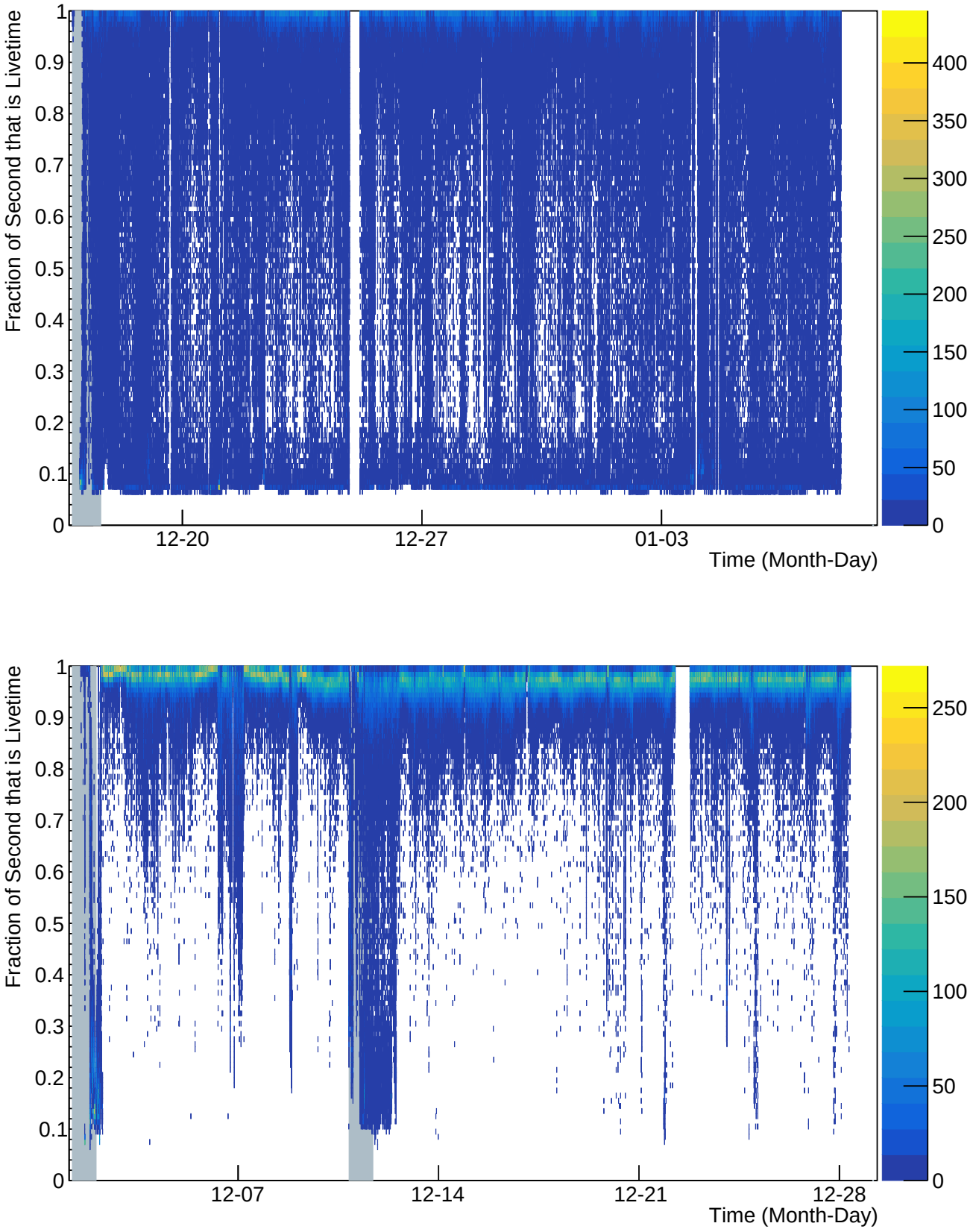

FIG. 13: Digitization livetime for ANITA-III (top) and ANITA-IV (bottom) reported as a fraction of one second. CW signal and problematic phi-masking were responsible for the persistent and large variation in livetime throughout the ANITA-III flight.

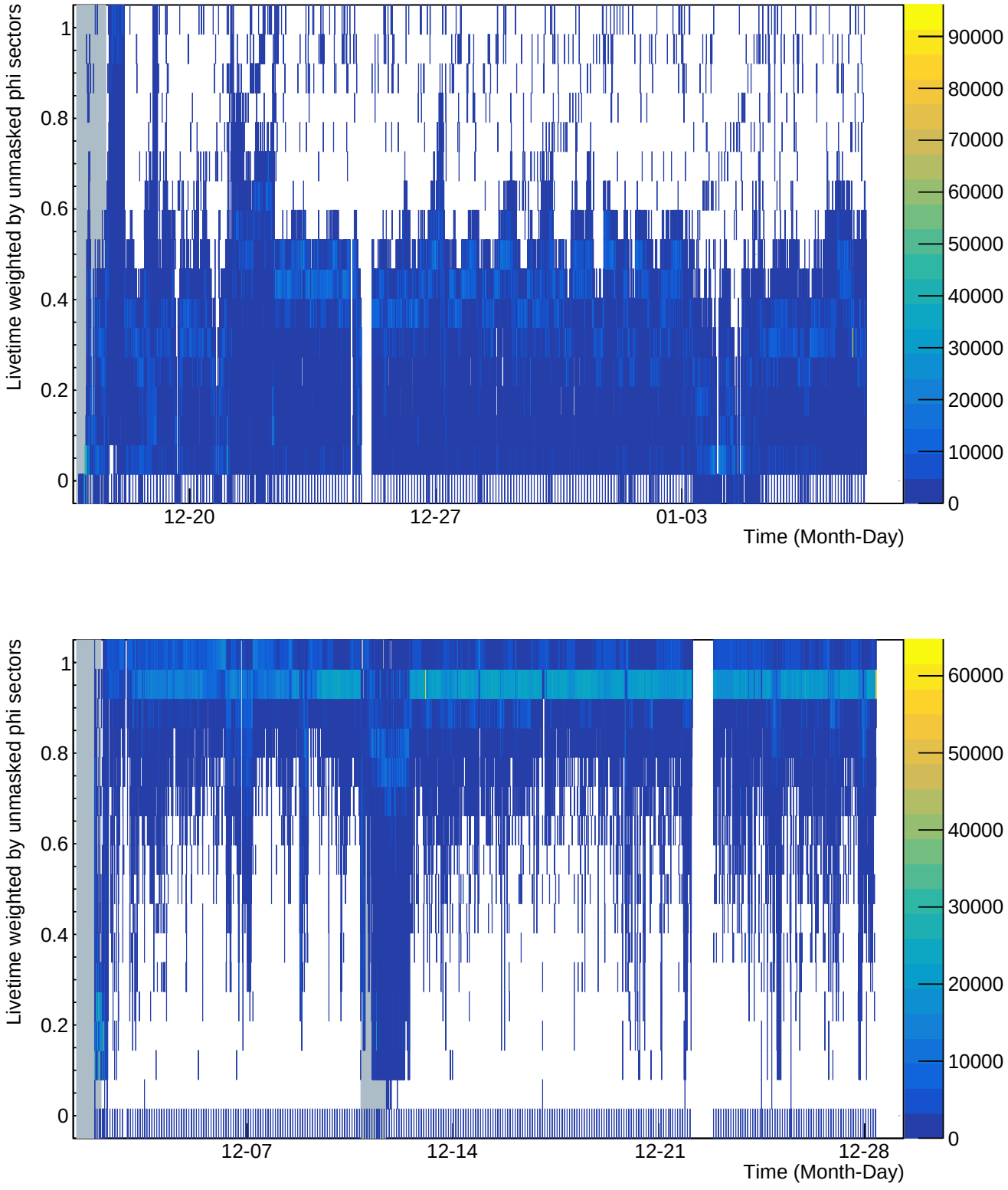

FIG. 14: Instrument livetime per second obtained by weighting digitization livetime by fractional unmasked phi sectors, for ANITA-III (top) and ANITA-IV (bottom).